Batteryless Bluetooth Low Energy Prototype With Energy-Aware Bidirectional Communication Powered by Ambient Light

Ashish Kumar Sultania and Jeroen Famaey, *Senior Member, IEEE*

***Abstract*—With the emerging deployment of Internet of Things devices, the industry is moving toward batteryless, maintenance-free, and sustainable solutions. Energy harvesting from ambient sources becomes crucial to support the uninterrupted execution of such applications. We choose the Bluetooth Low Energy (BLE) mesh network to analyze a batteryless node using the BLE Low power node (LPN) feature. We develop a prototype using a mini photovoltaic solar panel for indoor light harvesting using sunlight or a light bulb to power the BLE LPN. Due to the unpredictability of energy harvesting and the use of a small capacitor instead of a battery, the BLE LPN's power can become intermittent. This causes the device to frequently switch between the ON and OFF states as it is unaware of its available energy while trying to perform scheduled tasks. In contrast, an energy-aware LPN can try to avoid the OFF state. With the knowledge of the capacitor voltage, it can proactively delay the execution of upcoming sensing or communication tasks and provide some time to recharge the capacitor while consuming a minimum amount of energy by switching itself to the SLEEP state. This article presents the developed prototype and evaluates an energy-unaware and -aware batteryless BLE LPN communicating uni-directional downlink only or bi-directional for different capacitor sizes at different light-harvesting powers. The experimental results conclude that the energy-aware batteryless LPN performs better for both uni- and bi-directional communication with improved DL data latency up to 74% and avoiding restarts.**

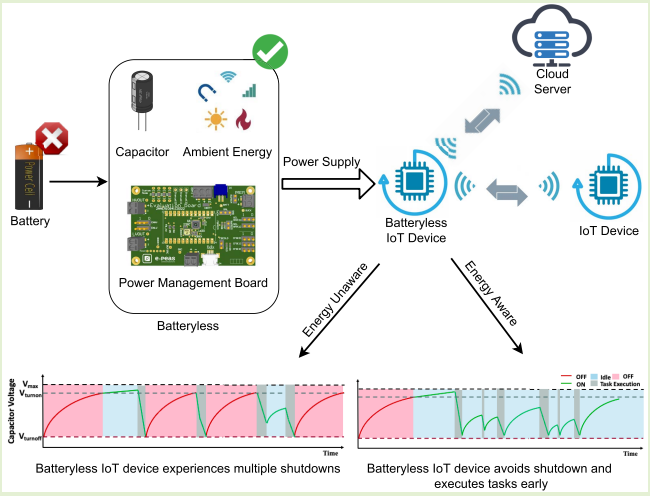

***Index Terms*— Batteryless node, bluetooth low energy, energy-aware node, low power node.**

I. Introduction

THE growing number of device deployments in Internet of Things (IoT) systems increases their maintenance cost. Thus, the market is motivated to develop 'deploy and forget' solutions [1]. Energy harvesting is targeted to either increase the lifetime of deployed devices by recharging the batteries or possibly the use of a self-sustaining energy source with a nearly infinite lifetime. This also reduces energy waste while decreasing the maintenance time and costs to replace batteries. Because batteries are bulky, expensive and can only support a limited number of charge/discharge cycles, they can be replaced with capacitors to store the harvested energy. This stored energy can be later used to power the sensor nodes [2]. Therefore, the interest in energy harvesting from ambient sources has been rising, enabling the Internet of Batteryless Things (IoBT). Renewable energy sources such as solar, wind, thermal, and radio frequency energy are popular options for harvesting. However, based on the harvesting power, availability and easy accessibility, light energy has emerged as the most popular harvesting approach for indoor IoT devices [3].

The communication protocols should handle IoT requirements such as support for low-power devices, operation in real-time, or support a large number of devices. Bluetooth Low Energy (BLE) is one of the most popular communications

Manuscript received February 2, 2022; accepted February 14, 2022. Date of publication February 21, 2022; date of current version March 31, 2022. This work was supported in part by the imec Interdisciplinary Cooperative Research (ICON) Project BLUESS, in part by the University of Antwerp Industry Research Fund (IOF) Funded Project COMBAT (Time-Sensitive Computing on Batteryless IoT Devices), and in part by the Flemish Fund for Scientific Research (FWO) Strategic Basic Research (SBO) through the Sustainable Internet of Batteryless Things (IoBaLeT) Project S001521N. The associate editor coordinating the review of this article and approving it for publication was Prof. Kazuaki Sawada. *(Corresponding author: Ashish Kumar Sultania.)*

The authors are with the IDLab, Department of Computer Science, University of Antwerp—imec, 2000 Antwerp, Belgium (e-mail: ashishkumar.sultania@uantwerpen.be; jeroen.famaey@uantwerpen.be).

Digital Object Identifier 10.1109/JSEN.2022.3153097

technologies for indoor applications due to its low power consumption and simplicity [4] that satisfies many IoT requirements. BLE allows many-to-many communication with its mesh specifications. This specification [5] categorizes the nodes as a relay, proxy, friend, or low power node (LPN). As a BLE mesh is broadcast-based, BLE nodes must always scan incoming channels, keeping their radio always on. This results in high power consumption, which a battery powered or batteryless node cannot cope with. On that account, BLE mesh supports a friendship feature for such LPNs to establish a relationship with a powerful single-hop reachable node called the *Friend Nodes (FN)*. The FN and LPN have a friendship relationship where the FN receives and temporarily buffers the DL data packets in a friend queue (FQ) intended for the associated LPNs while they sleep or temporarily shut down. And to receive the downlink (DL) data, LPNs have to poll the friend node (FN), which temporarily buffers the DL data. The polling happens periodically (based on a predefined duty-cycle) to receive any incoming data packets. This can reduce the overall energy consumption but increases the DL latency. However, LPNs can broadcast uplink (UL) data packets at any time and therefore, has less impact on UL latency. A node cannot have the low power feature enabled unless a neighbouring node agrees to be a friend. The friendship procedure can be visualized as two steps, namely, friendship establishment and message exchange. The establishment is initiated by the LPN sending the request to the neighbouring nodes (within a single hop) with the requirement of supporting a minimum time for ReceiveDelay (RD) and PollTimeout (PT). The neighbouring nodes can respond for the acceptance with their capabilities to become a friend with the supported ReceiveWindow (RW) value and their queue size. RD is the delay between the LPN sending the Friend poll (FP) message and when it starts listening to a response from the FN. The PT is used as a timeout to ensure that the friendship relationship is not kept alive indefinitely when an LPN leaves the network. During RW, the LPN expects the data and listens actively for it. After friendship establishment, the LPN periodically sends an FP message to the FN to get any stored data and keep the connection alive. The FP messages are sent in all the three BLE advertising channels (37–39). After receiving the FP message, the FN replies with the oldest buffered data packet. It discards the packet from the FQ once the LPN acknowledges its reception. If the FQ is empty, the FN responds with a friend update (FU) message. More details about the friendship message exchanges can be found in [6]. By considering the low energy consumption and the possibility of turning off the LPNs, they can be powered by harvesting energy from ambient sources.

A small (few mm^2) indoor solar panel based on photovoltaic (PV) cells can be utilized to harvest energy from light to persistently powers the BLE LPNs. Extracting energy from indoor sunlight makes the operation inherently dependent on the non-deterministic and variable weather conditions. When the harvested power is low, the instantaneous harvested power is usually insufficient for the IoT operations; the energy needs to be accumulated in the capacitor before starting the operations. Moreover, the capacitors have lower energy density and higher leakage current, so they cannot store a large amount of energy for a longer time interval. Therefore, the LPN can consume the stored energy in the capacitor much faster than it charges. This makes the LPN intermittently turn on and off.

As such, the LPN can work being either unaware of available voltage at its capacitor or being aware of it. An energy-aware LPN can avoid such intermittent behaviour by executing the tasks only if it has the required energy stored at the capacitor to execute the task. On that account, the energy-aware LPN delays the execution time of the task until its capacitor recharges up to a required threshold voltage. Therefore, the LPN operating as a batteryless node can experience an additional increase in data latency using both the solutions. This paper analyzes both the solutions with the integration of indoor photovoltaic (PV)-based energy harvesting capabilities to power the BLE LPN for the deployment of long-life and self-sustained solutions. In order to have predictable results, we analyze the batteryless BLE LPN prototype by harvesting from an indoor LED light placed at different distances (to adjust the harvesting power (HP)) of the solar panel.

The outline of this article is as follows. In Section II, we provide an overview of the related literature. The prototype design is presented in Section III, and Section IV presents the comparison of the energy-unaware and aware LPN. Finally, the conclusion is drawn in Section V.

II. Related Work

There are already some solutions that explore energy harvesting to enable batteryless BLE solutions. Various types of energy have been utilized, such as radio frequency (RF), solar, water, and wind energy. The batteryless BLE prototype, presented by Radhika *et al.* [7], is based on the ambient FM band and the dedicated BLE RF source. The solution enabled the UL data packet communication at an interval of 1,200 s harvesting from the FM band and at 90 s with the dedicated RF source. However, using a BLE device equipped with a 50 mF capacitor harvesting from a 5 m apart GSM mobile, Sanislav *et al.* [8] were able to support a data interval of 30 s.

Fraternali *et al.* [9] explored the design space of batteryless sensor nodes using commercial off-the-shelf components harvesting from ambient light. They study the BLE node lifetime, quality of service and energy availability for different capacitor sizes under varying lighting conditions. Meli *et al.* [10], [11] demonstrated the ability to execute the BLE protocol using a batteryless node. They showed that the batteryless BLE devices powered by a small solar cell in an indoor environment could sense the data such as temperature and humidity, which can later be sent to other nodes in the network. Wu *et al.* [12] also evaluate the performance of a subcutaneous solar energy harvester using a batteryless BLE prototype with a temperature sensor. Jeon *et al.* [13] proposed design principles for an ambient light energy harvesting BLE beacon capable of perpetual operation in an indoor environment based on the Nordic-nRF51822. Jang [14] investigated the output of the power management board (PMB) for a BLE node that harvests power from light using small capacitors of 200 μF and 420 μF. He founds that by increasing the advertising interval or the

capacitance, the number of charge-discharge cycles decreases. But he considers a prototype where the PMB starts charging the capacitor only when the solar panel output is higher than 1.55 V. He also conducted a similar study based on piezoelectric harvesting technology [15].

Other harvesting techniques are also used to design a batteryless BLE prototype. Zhong *et al.* [16] implemented their design of an implantable batteryless bladder pressure monitor system that monitors bladder storage in real-time and transmits the feedback signal to an external receiver through BLE. They use a four-coil wireless energy transmission method, which supports a power transmission range of up to 7 cm. A scalable solution is designed by Witham *et al.* [17] to detect water leakage using a batteryless BLE beacon powered by a customized sensor. Using a small capacitor of 3.9 mF and harvesting peak short-circuit harvesting current of 8.1 mA, the design was able to advertise data packets at an interval of 100 ms.

All the mentioned works focus on batteryless BLE applications that only target UL communication such that whenever the device harvests energy, it turns-on and sends the data periodically until it turns-off again. In contrast, our work studies the ability of a batteryless device to receive DL data and also having bi-directional communication using the friendship feature of the BLE mesh protocol. We chose commercial off-the-shelf components to design our prototype.

We analyse the energy-unaware and aware solution for a bidirectional BLE LPN communication. An energy-aware approach for a batteryless wireless sensor node (WSN) was first demonstrated by Ruan *et al.* [18]. They designed a custom prototype and interface that help the WSN to behave intermittently based on the defined capacitor voltage thresholds. They solve the WSN start-up problem which occurs due to the use of a power management system that supplies variable voltage directly from the capacitor. We use the similar concept of executing tasks in the batteryless node. However, we instead use an advanced power management board (Epeas-AEM10941) [19] that equalizes the supply voltage, and only provides the device with power if the capacitor voltage is within certain minimum and maximum bounds. Therefore, in our work, we are able to power on the energy-unaware node and able to compare its performance with the energy-aware node. There are also other works that consider the concept of energy-aware nodes such as [20], [21] but they consider batteries as the energy storage system. All these works consider only UL unidirectional data communication whereas our work support both unidirectional and bidirectional communication. The contributions made in this paper include 1) investigation of hardware components; 2) design principles for selecting hardware components subject to varying environmental conditions and application requirements; 3) prototyping to prove its practicality; and 4) analyze the energy-unaware and aware solution.

III. Energy Harvesting Prototype Setup

This section describes our prototype setup, including the selection criteria of hardware. The sustainability of the solution is evaluated by firstly measuring the amount of energy that can be harvested by a solar panel and later the power consumption of the BLE device executing an optimized LPN application. The power consumption of the application running on a BLE device is measured using off-the-shelf the Nordic-Power Profiler Kit-II (PPK-II), which has a resolution of 0.1 μA [22]. Moreover, the harvesting power at different indoor conditions is calculated by measuring the maximum power point (MPP) voltage V_{mpp} of the panel (maximum voltage that the panel produces with a load) and the MPP current I_{mpp} of the panel (maximum current that the solar panel produces). This is done by using the digital multimeter (Keysight-U1281A). Now, we will discuss the chosen commercial components and the reasons for each of them.

A. Hardware Trade-Off Analysis

- *Solar Panel:* The solar cells produce voltage and current when they are exposed to light. There are different types of solar cells available in the market, as classified by their materials, that can be used for IoT indoor applications. These materials are mono-crystalline, poly-crystalline, amorphous silicon, and concentrated PV. A common way to compare solar cells is by their efficiency, which measures how much of the power of the incident light can be extracted while working at the MPP. The concentrated PV cells have the highest efficiency, but they need a cooling system to achieve that. Therefore, mono-crystalline solar panels can be chosen for indoor IoT solutions, considering their high efficiency and life. We chose ANYSOLAR-SM141K06L 6-cells mono-crystalline panels which have a maximum efficiency of 25% at a reasonable cost. These solar panels are small and can supply up to 184 mW of power which is adequate to support BLE activities.
- *Light source:* Two different rooms whose corresponding windows are faced towards east and west are chosen. The sunlight in the room can be blocked by walls or furniture and thus does not distribute equally in the room. Therefore, the windowsill is chosen to place the solar panel to receives maximum light from the outside sun. As the sunlight intensity is unpredictable, we chose artificial lights placed at some distance from the solar panel to evaluate the performance in a controllable setup. There are various light sources available in the market, such as LED, Fluorescent, and halogen. LED has better luminous efficacy than Fluorescent [23]. Therefore, we selected a 6 W Warm White LED lamp (400 lm) from the Ikea-LED1521R6 series. The experiment with an artificial light bulb is conducted in a dark room where only the bulb produces the light.
- *Energy Storage:* The capacitance of supercapacitors, also known as electrochemical double-layer capacitors (EDLCs), ranges from a few mF to over 1000 F to store energy. Although their energy density is lower than that of batteries, they support many charge and discharge cycles, which in turn provides long life. Yet, they experience ageing effects, as with time, the Equivalent Series Resistance (ESR) increases, and its capacitance decreases. Furthermore, a supercapacitor does not work

TABLE I
EPEAS-AEM10941 BOARD CONFIGURATIONS

Config. no.	V_{max}	V_{turnon}	$V_{turnoff}$	V_{HOUT}	V_{LOUT}
1	4.50 V	3.67 V	2.80 V	2.5 V	1.8 V
2	4.50 V	3.92 V	3.60 V	3.3 V	1.8 V
3	4.12 V	3.67 V	3.01 V	2.5 V	1.8 V
4	4.12 V	4.04 V	3.60 V	3.3 V	1.8 V
5	4.12 V	3.67 V	3.60 V	3.3 V	1.8 V
6	3.63 V	3.10 V	2.80 V	2.5 V	1.8 V
7	2.70 V	2.30 V	2.20 V	1.8 V	1.2 V

ideally, as a high ESR limits the amount of useful energy that can be extracted once stored. Therefore, we chose the capacitors with the lowest ESR available in the market at an inexpensive price. The ESR of the supercapacitor is usually decreased with the increase in capacitance. The capacitors we chose have an ESR of 0.47Ω (for 0.47 mF), 0.22 Ω (for 1 mF) and 300 Ω (for 10 mF).

- *Power Management Board:* PMBs have multiple roles in the circuit. They are not limited to charging the storage, regulating the output voltage to the load, and extracting maximum power from the solar cell. Usually, due to the non-continuous and low ambient light source energy harvested by the solar panel, there is a need to use a PMB to manage this incoming power. The PMB can use a Maximum power point tracking (MPPT) circuit to collect as much energy as possible from the energy harvesters. It uses a boost converter to step-up the incoming DC voltage and a buck converter to step-down to a lower voltage. The Epeas-AEM10941 board is capable of both stepping up and stepping down a DC voltage. The stored energy is then converted to a stable voltage to operate a BLE board. The AEM10941 can be configured to supply different stable voltages (1.2, 1.8, 2.5 or 3.3 V) as V_{HOUT} and V_{LOUT}. The cold-start voltage, i.e., the voltage needed at the start of the capacitor charging, is by default at its minimum value of 380 mV with an input power of only 3 μW.
  The PMB can charge up the capacitor maximum up to a certain voltage level (V_{max}) and can release the stored energy whenever required by the end-node. The PMB also manages the lower threshold of the capacitor by cutting off the output to the end-node once its voltage drops to $V_{turnoff}$ and can release output when the voltage of the capacitor increases to V_{turnon}. The Epeas AEM10941 board already supports seven different configurations as defined in Table I. The user can also define its configuration but needs to add extra resistors to the board.
- *BLE board:* There are many boards available commercially to build BLE Mesh applications, and their energy consumption comparison can be found in [24]. With the lower energy consumption, and the support of Software Development Kits (SDKs) (containing all the Bluetooth software, structure and Mesh protocol), example applications (to test the device) and online community, Nordic boards are chosen to develop batteryless applications. We chose the Nordic nRF52840 DK board [25]. The boards can be programmed to behave like a node in a Bluetooth Mesh network and act as a relay node, FN or LPN. It can be powered by the Epeas-AEM10941 V_{HOUT} or V_{LOUT} in the range greater than 1.8 V.

B. Energy-Unaware and -Aware LPN

When the capacitor voltage drops below a turn off voltage ($V_{turnoff}$), the node turns off as shown in Figure 1, as such, the LPN can work being either unaware of the available voltage at the capacitor or being aware of it. This intermittent behaviour can be observed more in an energy-unaware solution because the batteryless device will try to execute the tasks as soon they are scheduled. As shown in Figure 1a, during the execution of Task 2 and Task 3, the capacitor's voltage drops below $V_{turnoff}$, and the device loses power. This forces the device to reschedule these tasks upon the next wake-up time (i.e., the task execution was delayed until the capacitor again reaches V_{turnon} voltage). However, the device can avoid this with an energy-aware solution by checking the capacitor voltage before executing any task. The batteryless device should start the task only if its capacitor has acquired a sufficient threshold voltage ($V_{threshold}^{Task_i}$) corresponding to that task ($Task_i$) and should not drop its voltage below a cut-off voltage V_{cutoff} after the execution. The cut-off voltage should be selected above $V_{turnoff}$ to ensure the LPN avoids turning off. However, if its voltage is below the required threshold value, it can periodically check the available voltage at a fixed energy check interval (ECI). Figure 1b shows such behaviour, where to execute Task 3, the device wakes up twice to check the energy. Intrinsically, energy-aware solutions can have a great potential to improve network performance. Comparing both the solutions in Figure 1, it can be possible that the energy-aware solution executes more tasks within the same time interval. However, it is needed to spend a small amount of energy to check the voltage of the capacitor. Therefore, the ECI should be selected optimally so that the device does not end up spending energy only to check the voltage rather than to execute the scheduled tasks.

C. LPN Application Implementation

The application development is based on the Nordic software development kit (SDK) for Mesh v.4.2.0 and corresponding SoftDevice v7.0.1 with the SDK version 16.0.0. Firstly, to develop the application for a batteryless LPN application, we add a vendor-specific mesh model to send string messages. This helps to communicate any message, such as temperature, event detection, humidity, etc., on the same destination group address using a single model. The receiver end can decode the messages based on the first character in the string message. Secondly, being a batteryless node, it can shut down unpredictably due to the unavailability of energy. Thus, we modify the SDK's Application Programming Interfaces (APIs) so that the LPN saves the context of the associated FN during the friend establishment phase in the free pages of the flash memory. On the restart, the LPN reads the flash data, and if the FN context is already saved in a

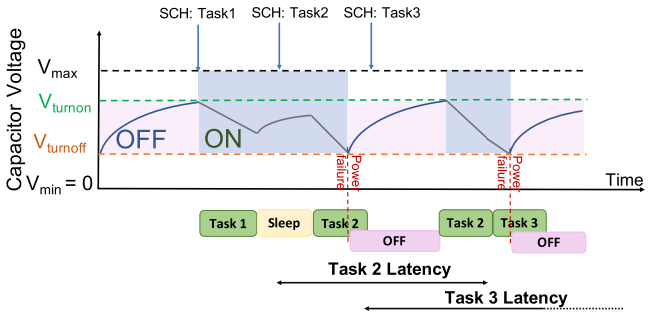

(a) Energy-Unaware

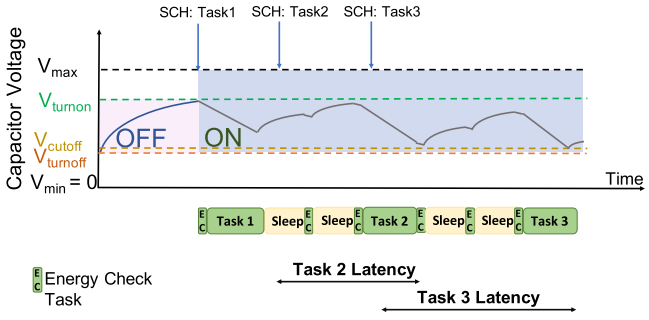

(b) Energy-aware

Fig. 1. Comparing energy-unaware and aware solution.

flash, the LPN restores the local friendship context without reassociating. Furthermore, we divide the usage of the PT timer into polling interval timer (T_{PI}) and poll expiration timer (T_{PE}). According to the specification, the PT timer is the time between two consecutive requests sent by the LPN, and if the FN receives no FPs before the expiration of the PT timer, then it assumes that the LPN is disconnected from the network. Thus, the FN can consider that the termination of the friendship. The batteryless LPN can stay in a turnoff state for a long time and should stay connected to the FN without such restriction. Accordingly, the LPN should try to poll on every expiration of T_{PI} and the FN should consider the termination only on the expiration of T_{PE}.

Moreover, we extend the *lpn* [26] and *light_switch* [27] examples provided in the Nordic SDK. We optimize the *lpn* example such that it consumes as low energy as it can. We enable DC/DC regulators to maximize the system's power efficiency. The *light_switch* example is modified to respond to the incoming messages in its vendor model. A USB powered Nordic device runs the *light_switch* example to act as a friend node, whereas the capacitor enabled PMB supplies power to the node running the modified *lpn* example.

D. Energy-Aware System

An Analog-to-digital Converter (ADC) pin of the Nordic board can be leveraged to read the capacitor voltage. However, the capacitor can not be connected directly to this Nordic DK pin due to two reasons. First, the capacitor can supply a burst of current to this pin that could damage the device and second, the Nordic DK can read inputs only up to the maximum operating voltage. Therefore, the solution is to have a voltage divider that can reduce both the current and voltage.

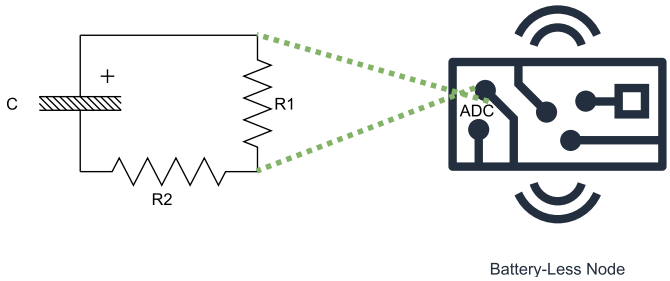

Fig. 2. Voltage divider circuit.

The schematic diagram of the voltage divider circuit [28] is shown in Figure 2. The resistors need to be selected such that the voltage entered from $R1$ should be in the range permissible by the Nordic board. The output voltage is based on Ohm's law and calculated as Equation 1.

$$V_{R1} = \frac{V_c \times R_1}{R_1 + R_2}, \tag{1}$$

where, V_{R1} is the input voltage to the board, V_c is the actual capacitor voltage, and R_1 and R_2 are the resistance of the resistors.

Now, depending on the bit size of the ADC, the measured ADC value can be converted to the actual voltage of the capacitor. For example, for an N bit ADC, working at a standard operating voltage of V_{op}, the formula to convert is mentioned in Equation 2.

$$V_c = \frac{V_{op} \times N_{adc}}{2^N}, \tag{2}$$

where, N_{adc} is the digital value on the ADC pin.

Moreover, to reduce the continuous current consumption due to the added resistors, MOSFETS are used as a circuit switch. An N-channel MOSFET can close the circuit when a positive voltage is applied to its gate from a GPIO pin of the Nordic board. By connecting this additional circuit to the Nordic DK board, the LPN application can be modified to act based on the measured voltage of the capacitor and become energy-aware. The harvested energy can be better used by determining the usable energy stored in the capacitor [18]. However, the LPN needs to define the thresholds of its tasks in the application.

The voltage (energy) function of a capacitor supporting various tasks is introduced by Sabovic et al. [29]. Equation (3) provides the initial voltage on the capacitor before the device operates at a load current of $I_L(X)$ (amperes) in the state X for a time Δt harvesting from a constant current source providing the current of I_h (watts).

$$V(t) = \frac{V(t+\Delta t) - I_h \cdot (E/I_L(X)) \cdot (1 - e^{\frac{-\Delta t \cdot I_L(X)}{E \cdot C}})}{e^{\frac{-\Delta t \cdot I_L(X)}{E \cdot C}}}. \tag{3}$$

The threshold voltage for each task X of an LPN with a capacitor size C can be calculated by deducing $V(t)$ considering $V(t+\Delta t)$ as $V_{turnoff}$ and putting the correct values of I_h and I_L. This would be a simplified approximation because the harvester, such as solar panels are not ideally a constant current source.

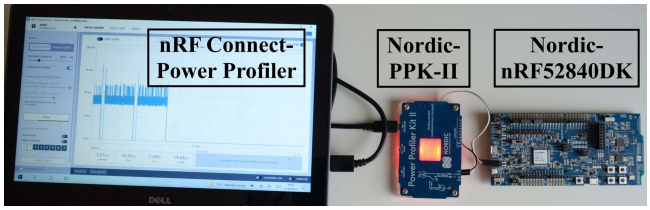

Fig. 3. Nordic PPK-II connection.

TABLE II
POWER CONSUMPTION AT $V_{op} = 1.8$ V

State	Average Current Con. (mA)	Time (ms)	Average Power Con. (μW)
Initialize	2.25	5.431	21.99
Flash Read (Check FN Context)	5.01	25.61	230.94
Flash Write	4.54	7.155	58.46
Rx Data	4.15	4.207	31.42
Rx FU	4.02	3.669	26.53
Rx FO	4.80	3.495	30.186
Tx Data	3.18	4.01	22.95
Tx FP	3.5	3.841	24.19
Tx FR	3.61	4.098	26.62
Tx FP + Rx Data	0.315	104.7	59.36
Tx FP + Rx FU	0.297	104.5	55.85
Tx FR + Rx FO + Flash Write	0.577	110.2	114.44
Sleep State	0.00627	N/A	N/A

(a) Energy-unaware LPN

State	Average Current Con. (mA)	Time (ms)	Average Power Con. (μW)
Initialize	2.25	5.431	21.99
Flash Read	5.41	24.66	240.14
Flash Write	4.53	3.314	27.01
Energy Check (EC)	4.86	2.583	22.59
EC + Tx Data	0.601	35.18	38.07
EC + Tx FP	0.695	29.33	36.68
EC + Tx FP + Rx Data	0.412	107.6	79.79
EC + Tx FP + Rx FU	0.379	107	73
EC + Tx FR + Rx FO + Flash Write	0.596	113.6	121.87
Sleep State	0.0062	N/A	N/A

(b) Energy-Aware LPN

E. Computing BLE LPN Power Consumption

To be able to calculate the voltage threshold of each application task X using Equation 3, we thus need to know the load current $I_L(X)$. We use the Nordic PPK-II connected with the Nordic board in source meter mode as shown in Figure 3 to measure the current consumption of each application task. The Nordic board executes in `nRF Only` mode, which reduces the current consumption by shutting the power supply to several external components such as external memories, LEDs and buttons. The Nordic PPK-II interface provides the graphs in real-time, and the data can be exported to a CSV file. We observe that the lower the supply voltage, the lower the power consumption. Moreover, as Epeas V_{LOUT} pin can be configured to 1.8 V, and that is in the range of the operating voltage of the Nordic board, we use 1.8 V to measure the current consumption. Based on the measurements, the power consumption for different states of the LPN is presented in Tables IIa and IIb. The voltage divider circuit with MOSFET and a large resistor are always connected to the Nordic board, which incurs extra current consumption in the energy-aware LPN. Moreover, the reported numbers are averaged over ten different executions. These numbers vary, with around 8% of deviation on different executions due to the erratic behaviour of hardware. It can be noted from Tables IIa and IIb that flash activities are power-consuming tasks and therefore should be avoided as much as possible. In our application, flash write is performed only when the friendship is established, and flash read when the LPN is rebooted to restore the FN context. To summarize, the unaware LPN performs more flash reads, as it often reboots, while the energy-aware LPN incurs more power consumption due to maintaining the sleep state and using the voltage divider and MOSFETs.

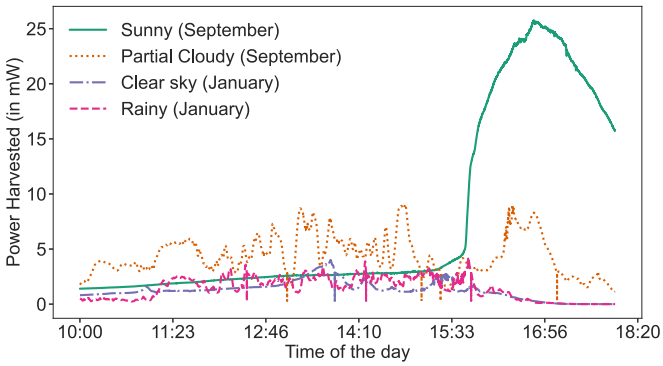

Fig. 4. Harvesting power using sunlight at west-side windowsill.

F. Computing Harvesting Power

In order to evaluate if indoor light harvesting can sufficiently power the LPN activities such as friendship establishment, message exchange, sensing, and reading/writing into flash memory, preliminary measurements to calculate the harvested power are performed. The Epeas board harvests power at MPP (P_{mpp}), which can be calculated by measuring MPP voltage (V_{mpp}) and MPP current (I_{mpp}). P_{mpp} is computed for different times of the day with sunlight and differently distanced light bulbs (in a room without sunlight). The calculated P_{mpp} for an entire day using the solar panel placed at a west-side windowsill is shown in Figure 4. It can be observed that during most of the time, the panel can easily harvest around 2 mW in January and around 3 mW in September. On a sunny day, when sunlight falls on the solar panel, the harvested power can be increased by eight times. Whereas, with artificial light (Figure 5), the harvested energy is more predictable and varies from 50 mW (10 cm) to 60 μW (210 cm).

It is also observed that the harvesting power is lowest during the winter months (October to February), and the average is usually less than 6 mW. This is equivalent to harvesting the energy from a LED bulb placed 20 to 30 cm away from the panel. It should be noted that the source light spectrum is also not analyzed. When sunlight shines through the windows of a building, it also loses some of its energy because glass windows typically block UV radiation [30]. Therefore, based on the type of window glass used, the results can deviate.

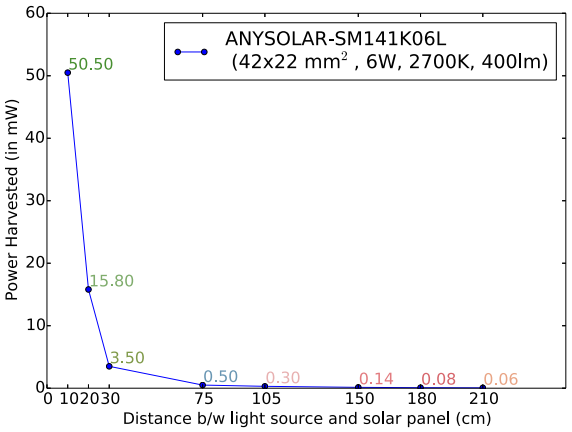

Fig. 5. Harvesting power using light bulb.

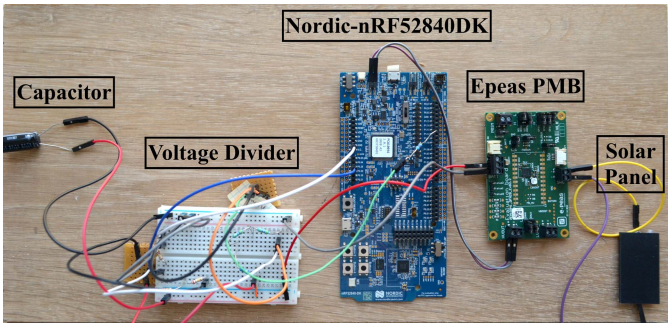

Fig. 6. Energy-aware prototype setup.

G. Final Prototype Design

The setup of the batteryless prototype for an energy-aware solution is shown in Figure 6. Whereas, for an energy-unaware solution, the voltage divider is removed. The Epeas-AEM10941 evaluation board is attached to the solar panel and a supercapacitor. One of the output pins of the board provides power to the Nordic nrf52840 DK. Figure 7 shows the flow chart of the LPN's execution. The LPN's application starts by initializing its memory and BLE mesh stacks. In an energy-unaware solution, it works intermittently due to unpredictable energy sources and storage for the scheduled tasks. Thus, upon power failure, the volatile memory is lost. Therefore, some data (e.g., the context of the associated FN) needs to be retrieved from non-volatile memory after regaining power. Therefore, the LPN checks its flash memory for the saved context. If the context is present, the LPN starts the polling process. Otherwise, it starts the friendship establishment followed by saving the friend context in flash memory. This retrieval for the Nordic board is done by reading the FN context from the flash memory, which itself is a power-hungry task. This lowers the overall usable energy to perform BLE computations. Thus, the energy-aware solution can benefit as it avoids restarting by making intelligent decisions to delay the tasks' execution by checking the capacitor voltage before executing any tasks. Also, large size capacitors can store more energy, but their charging time is higher. An LPN with a large capacitor harvesting at a low HP can take hours to charge the capacitor from $V_{turnoff}$ to V_{turnon} (for unaware LPN) or from V_{cutoff} to $V_{threshold}^{Task_i}$ (for aware LPN). During this time, the LPN is unavailable and therefore, there is a need to choose an

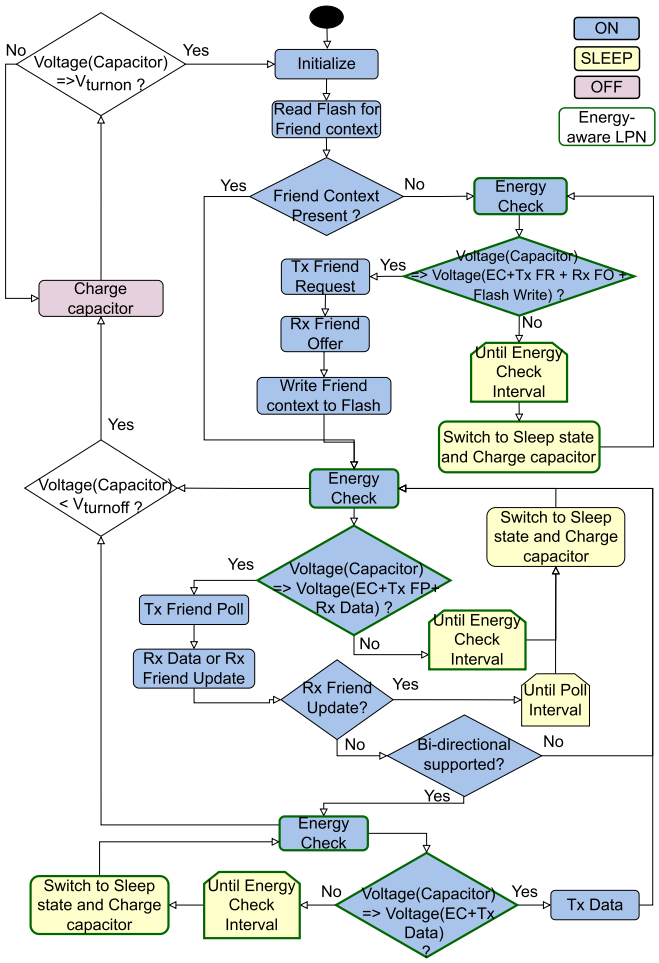

Fig. 7. Flow chart of LPN tasks.

optimal minimum size of the capacitor based on the required data interval (DI) and minimum available HR. We consider an LPN that attempts to receive DL packets, transmitted by a remote node, and buffered by its FN. Therefore, after the friendship establishment, it continuously sends FPs to retrieve these DL packets. Moreover, the LPN can also send UL packets without any dependencies on its FN. Therefore, if bi-directional support is enabled, the LPN also tries to send UL packets as well as receive DL packets.

As an unaware batteryless LPN can only operate during the time the capacitor discharges from V_{turnon} to $V_{turnoff}$; we choose the configuration number 1 of the Epeas board from Table I which provides the maximum difference in V_{turnon} and $V_{turnoff}$. In comparision, the aware LPN executes tasks once it attains $V_{threshold}^{Task_i}$ which needs to be calculated for each task. Based on the measured current consumption of each task (Table IIb) and the configured voltages, the corresponding threshold voltages are calculated using Equation 3 as presented in Table III for the selected Epeas configuration. The HP is considered to be low between 140 and 280 μW. This is sufficient to keep charging the energy-aware LPN's capacitor while the LPN is in the sleep state. As shown in Figure 7 if at any stage the capacitor voltage goes below $V_{turnoff}$, the LPN would be switched off and the capacitor will be charged. However, to choose the $V_{threshold}^{Task_i}$ for the energy-aware LPN,

TABLE III
THRESHOLD VOLTAGE FOR CONFIGURATION 1 (V_{max} = 4.5 V, V_{turnon} = 3.67 V, $V_{turnoff}$ = 2.8 V), HP = 140 μW, V_{cutoff} = 2.83 V

State	C= 0.22mF	C= 0.47mF	C= 1mF	C= 10mF
Initialize	2.87	2.85	2.84	2.84
Flash Read	3.23	3.01	2.92	2.84
Flash Write	2.88	2.85	2.84	2.84
EC	2.87	2.85	2.84	2.84
EC + Tx Data	2.88	2.86	2.84	2.84
EC + Tx FP	2.88	2.86	2.85	2.84
EC + Tx FP + Rx Data	2.92	2.87	2.85	2.84
EC + Tx FP + Rx FU	2.83	2.83	2.83	2.84
EC + Tx FR + Rx FO + Flash Write	2.98	2.9	2.87	2.84

V_{cutoff} is considered. V_{cutoff} (below which the energy-aware LPN would stop its tasks' execution) is chosen as $V_{turnoff}$ plus 0.03 V. By considering the response time of the Epeas PMB board to decide to shut down the voltage supply, we experimentally found that selecting V_{cutoff} of 2.83 V can avoid restarting the energy-aware LPN with the smallest capacitor size. These threshold values are in the range between V_{max} and $V_{turnoff}$; therefore, the aware LPN would be able to execute the tasks. The aware LPN can be configured to execute each task when the corresponding capacitor threshold voltage is reached based on the size of the attached capacitor. The threshold voltage of the small capacitor is higher than that of the large capacitor. Thus, for simplicity, we use the threshold of the lowest capacitor (0.22 mF) to execute the aware LPN application attached to any capacitor size of 0.22 mF or higher. While this is suboptimal for larger capacitor sizes, it allows us to use a single task scheduling configuration, independent of the used capacitor size and the Epeas configuration.

IV. COMPARISON OF ENERGY-UNAWARE AND -AWARE LPN

We set up two experimental use-cases to compare the energy-unaware and -aware LPN as follows:

- *Uni-directional DL only*: The LPN is expected only to receive data from other nodes in the mesh network that is being transmitted at a fixed interval.
- *Bi-directional communication*: The LPN is expected to receive data from other nodes in the mesh network, and upon receiving a data packet, it sends back a UL packet.

Each data packet is considered to be unsegmented with a fixed payload length of 8 bytes. Also, after the data communication, the LPN returns to sleep mode, consuming a minimum amount of energy (6.2 μA). Our work is focused on evaluating the friendship feature specifically, we omit the uni-directional UL only use case.

We consider the DI of 5 s. It is observed that when the data is transferred at a fixed DI of 5 s, the energy harvested with the light bulb at a distance of 105 cm (i.e., 300 μW) is sufficient for the operation of the LPN. Therefore, the sunlight in the daytime is also more than sufficient to support all the use-cases (Uni- and Bi-directional communications). At this HR, the voltage of the small capacitor (0.47 mF) never drops below, $V_{turnoff}$ and so the results in unaware and aware solutions are similar. As such, we analyze the batteryless LPN harvesting at rates lower than 300 μW in the remainder of this section.

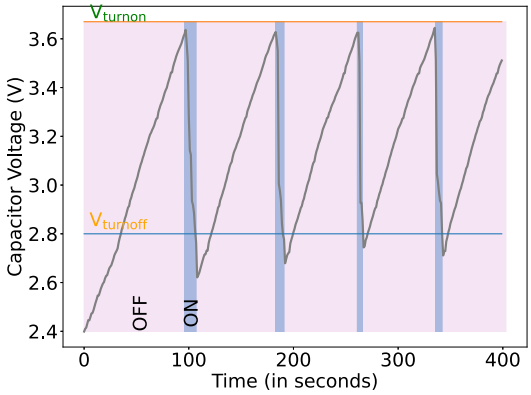

(a) Unaware

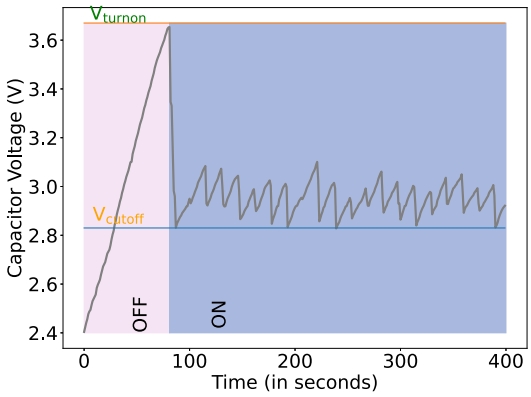

(b) Aware

Fig. 8. Variation in 0.47 mF capacitor voltage supporting bi-directional communication at 80 μW for Epeas Configuration 1, ECI = 15s.

A. Capacitor Voltage Behaviour

We compute the charging and discharging behaviour of a batteryless LPN for the energy-unaware and aware application. Figures 8-9 show, for a 0.47 and 1 mF capacitor, respectively, the variation in the capacitor voltage running the LPN application with bi-directional communication on a batteryless node harvesting at 80 μW for the Epeas configuration 1. It can be observed that the unaware LPN's capacitor voltage continuously goes below 2.8 V ($V_{turnoff}$) while doing the LPN's activities (flash read/write, polling, data communication), leading the PMB to turn off the LPN and later turning it on again at 3.67 V. The energy-aware LPN never goes below 2.8 V and recharges the capacitor up to the required threshold voltage to perform the LPN's tasks. The drop of the capacitor voltage does not stop strictly at 2.8 V because it depends on the action sensitivity of the Epeas PMB to stop supplying energy from the capacitor.

The LPN's outage time depends on the capacitor size and the active-time voltage gap. The larger the capacitor, the longer it takes to charge and discharge. By comparing Figures 8 and 9, it can be noted that the smaller capacitor causes more frequent charge-discharge cycles of the capacitor. The charging time from $V_{turnoff}$ to V_{turnon} for an unaware LPN that is supported by a 0.47 mF capacitor takes around 64 s, and

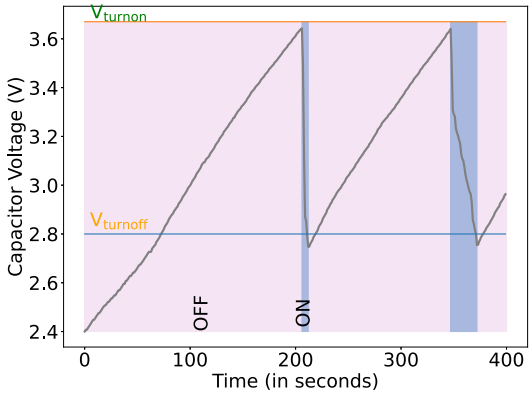

(a) Unaware

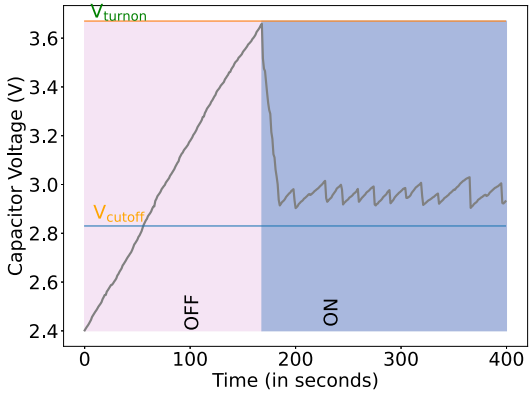

(b) Aware

Fig. 9. Variation in 1 mF capacitor voltage supporting bi-directional communication at 80 μW for Epeas Configuration 1, ECI = 15s.

stays on 10 s while performing communication. With a 1 mF capacitor, the active communication time increases to 25 s, but now the charging time also increases to 135 s. In contrast, once the aware LPN becomes active, it does not execute any tasks for the time to recharge the capacitor from V_{cutoff} to $V_{threshold}^{Task}$. When first turning on at a voltage of 3.67 V, the LPN spends energy in reading the flash and establishing a friendship with an FN. Later, there are mostly two activities scheduled, which are receiving DL by polling and optionally sending UL data. The average waiting time for an aware LPN with a 0.47 mF capacitor is 15.7 s which then receives and sends one data packet. However, with 1 mF, it only takes 12.7 s to recharge from its corresponding V_{cutoff} to $V_{threshold}^{Task}$. This is because of two reasons. First, voltage drop after task execution for a 0.47 mF capacitor is higher than that of a 1 mF capacitor. Secondly, for the first reason, the number of the executed energy check (EC) tasks of 0.47 mF capacitor is more than that of a 1 mF.

B. Result Analysis

The Epeas PMB is configured with configuration 1 to analyze the energy-unaware and aware LPN. The following performance metrics are considered in the comparison between the friendship communication mechanisms:

- *Average DL Data Latency*: The average time gap between receiving a packet by the LPN from the time it arrives at the FQ.

TABLE IV
OPTIMAL CONFIGURATION FOR ENERGY-AWARE LPN FOR DR = 5S

Traffic type	HP	FQ	Best Configuration(s) (CS,ECI)
Uni-directional	140 μW	16	(1mF, 20s)
	210 μW	16	(1mF, 5s), (0.47mF, 3s)
	280 μW	16	(1mF, 3s), (0.47mF, 3s)
	140 μW	8	(1mF, 5s), (0.47mF, 5s)
	140 μW	4	(1mF, 4s), (0.47mF, 5s)
	140 μW	2	(1mF, 4s), (0.47mF, 5s)
Bi-directional	140 μW	16	(1mF, 20s)
	210 μW	16	(0.47mF, 3s)
	280 μW	16	(1mF, 3s), (0.47mF, 3s)
	140 μW	8	(1mF, 30s),(0.47mF, 30s)
	210 μW	8	(1mF, 10s)
	280 μW	8	(0.47mF, 3s)

- *Average DL Data Inter-arrival Time (IAT)*: The average time difference between the arrival of two consecutive DL packets received by the LPN.
- *Average UL Data IAT*: The average time difference between the arrival of two consecutive UL packets received by the FN.
- *Discarded Packet Percentage*: The percentage of packets that are discarded from the FQ due to queue overflow.
- *Restart Count*: The number of restarts by the LPN.
- *Outage Time*: The time during which the LPN is in the OFF state.

1) Uni-Directional DL Only: Figure 10 shows the results for different ECIs for the LPN receiving data at 5 s data interval and harvesting at 140 μW. It can be observed that as the capacitor size increases, more packet drops can be observed. This is because the larger the capacitor, the more time it takes to charge. At an ECI of 20 s with 1mF capacitor, the energy-aware LPN shows the best DL data latency. With the same capacitor for the lower ECIs (less than 15s), the LPN wastes energy in checking the capacitor voltage frequently rather than initiating an FP. As a result, it delays the capacitor voltage in reaching $V_{threshold}^{DL}$. Therefore, the latency is higher than when using an ECI equal to 15s. Whereas, increasing the ECI beyond a certain value (20 s with 1mF or 10 mF and 25s with 0.47 mF) increases the delay as the device does not immediately detect the voltage threshold ($V_{threshold}^{DL}$) being reached. Therefore, the DL data latency and packet discard percentage increases for those large ECIs (can be observed with 10 mF). This can be confirmed by checking the capacitor charge time, which in these cases is equal to or close to the corresponding ECI. The capacitor charge time of the unaware LPN is high, but it can send more than 1 packet during its ON state. The best result of the unaware LPN is at 0.47 mF capacitor with no packet loss. As the developer can choose both the ECI and capacitor size, we will compare the optimal ECI/capacitor combination of the energy-aware solution, with the optimal capacitor size of the energy-unaware solution in the remainder of this section. Table IV shows all the optimal configurations for different traffic types, FQ sizes, and harvesting powers.

It can be observed from Figure 11 that the larger the FQ size, the better the energy-unaware LPN performs in terms

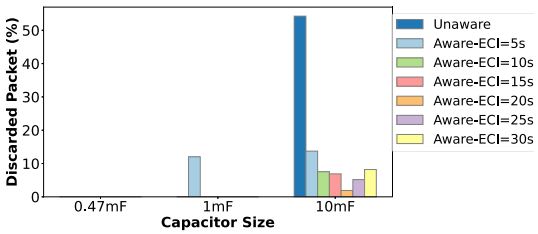

(a) Packet Discarded

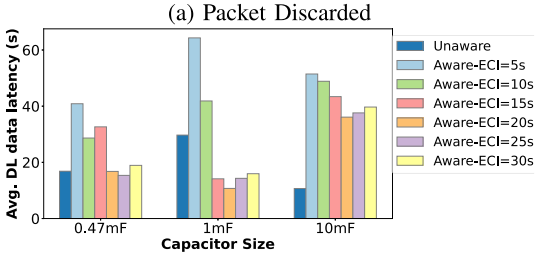

(b) DL data latency

Fig. 10. Uni-directional communicating LPN's performance for different ECI at HP = 140 μW and FQ = 16.

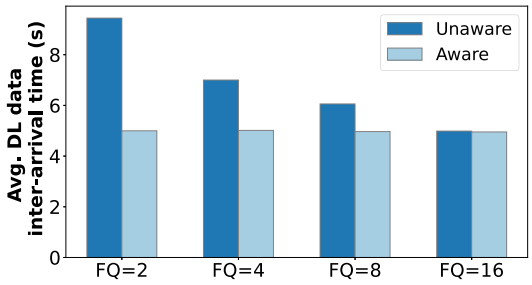

(a) DL data inter-arrival time

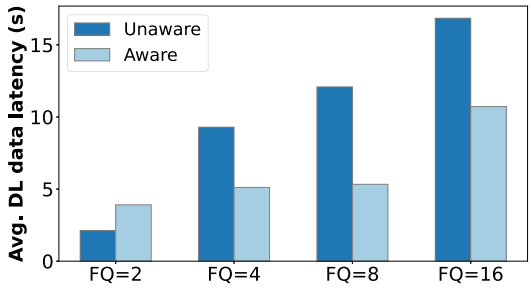

(b) DL data latency

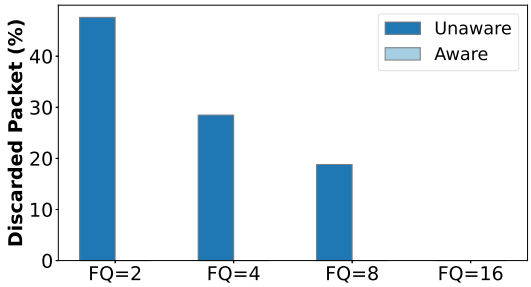

(c) Packets discarded

Fig. 11. Uni-directional communicating LPN's performance for different FQ at HP = 140 μW, Optimal ECI.

of IAT and discarded packets. As with the increase in FQ, more packets start being queued, the unaware LPN receives more packets per discharge cycle. Thus, the packet discard percentage is reduced. Also, several packets need to wait

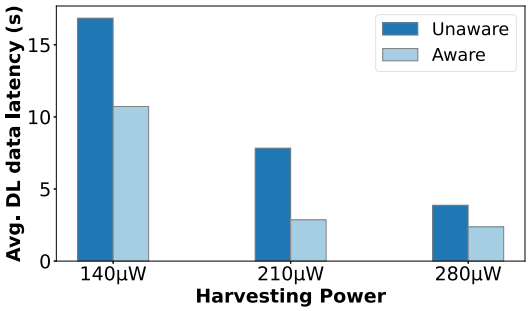

(a) DL data latency

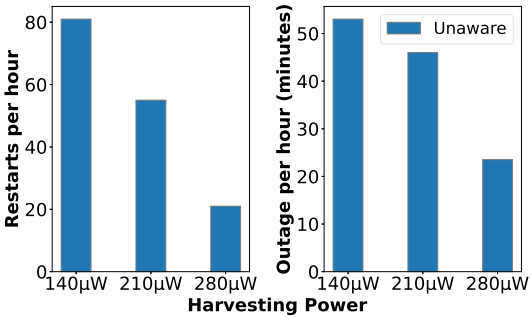

(b) Energy-unaware LPN outage

Fig. 12. Uni-directional communicating LPN's performance at different HP at FQ = 16, Optimal ECI.

longer to be polled by an LPN, which increases the overall DL data latency. It is the same for the aware LPN, which increases its DL data latency. However, the energy-aware LPN polls whenever it gains the threshold voltage to receive a DL packet ($V^{DL}_{threshold}$), which takes less than 5 s, and therefore it never receives an FU. Therefore, the discarded packet percentage and the IAT does not change. As at FQ equal to 16, the energy-unaware LPN shows zero discarded packets, we consider this FQ size to compare it with aware LPN results.

Further, an optimal ECI configuration is considered to send data at 5 s intervals, harvesting at different rates (140 to 280 μW) and having an FQ equal to 16. The results are shown in Figure 12. It is observed that the DL data IAT is 5 seconds for both the LPNs (energy-aware and unaware) for all the HPs, while there is no packet loss. However, as the harvested power increases, the capacitor charging time decreases, which decreases the DL data latency and also the number of restarts and outage time per hour. An energy-aware LPN gains the benefit of lower data latency, which is up to 63% at HP of 210 μW. Also, the energy-unaware LPN improves its performance for higher HP but still have DL data latency 38% higher than the energy-aware LPN. It also experiences outages due to restarts, which is 23.5 minutes per hour.

2) Bi-Directional Communication: The pattern of the bi-directional communication results is the same as uni-directional communication. When both UL and DL data are communicated, the LPN consumes a bit more energy in each cycle than uni-directional communication; therefore, the DL data IAT is increased. It can be observed from Figure 13a) that the DL data IAT is increased about 6% for an aware LPN harvesting at 140 μW. However, the UL data IAT for the

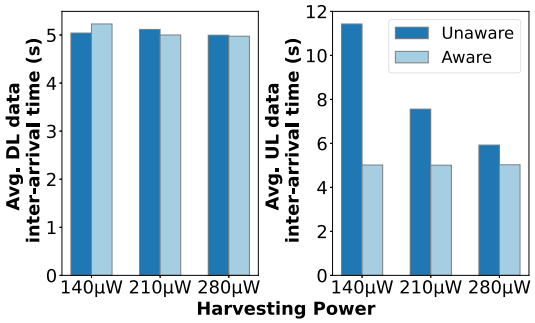

(a) Data inter-arrival time

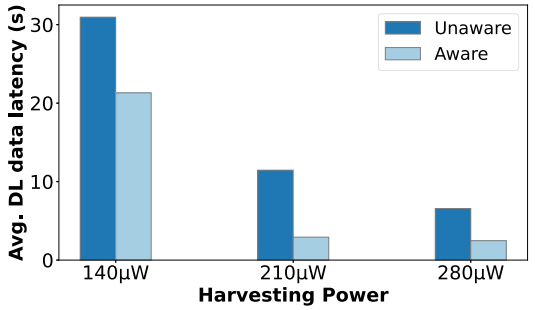

(b) DL data latency time

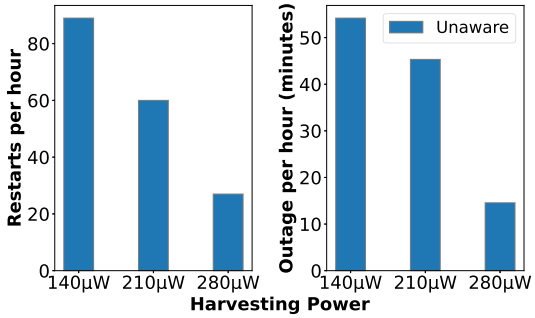

(c) Energy-unaware LPN Outage

Fig. 13. Bi-directional communicating LPN's performance at different HP at FQ = 16, Optimal ECI.

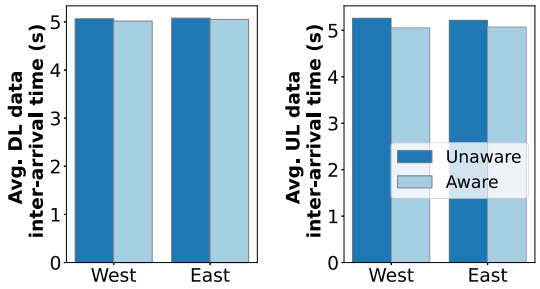

(a) Data inter-arrival time

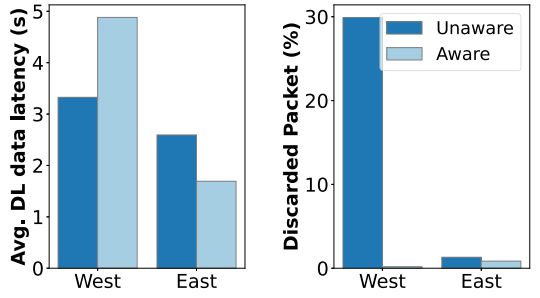

(b) DL data latency

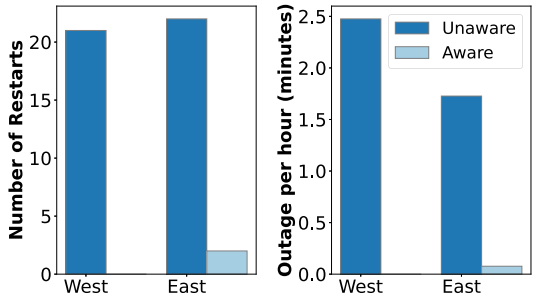

(c) LPN Outage

Fig. 14. Bi-directional communicating LPN's performance by placing solar panel at the east and west side windows.

aware LPN is better than unaware (more than half) because for UL, there is no buffer to store the packets temporarily. The DL data latency for the aware LPN is always lower than the unaware LPN. At the HP of 210 μW, the energy-aware LPN shows maximum improvement (up to 75%) on DL data latency over its counterpart. Furthermore, compared to uni-directional communication, the DL data latency for bi-directional communication is higher because of the power consumption due to the additional UL tasks. And for the same reason, the restart count and the outages increase a bit. The DL data discard percentage for the LPNs is zero (graph not shown).

3) Natural Light Experiments: We perform experiments using natural light to evaluate the performance of the system under dynamic harvesting power that changes over time. The setup is placed at the windowsills of two separate rooms in the east and west direction in Antwerp, Belgium, where the indoor sunlight is coming from the double-layered glass windows. The energy-aware LPN is equipped with a 1 mF capacitor, and the ECI is configured to 3s (the optimal configuration at 280 μW). On 21st Sept, the day was sunny, and the sun rose and set at 07:27 and 19:43, respectively [31]. The performance of both the LPNs placed by the east and west windowsills is presented in Figure 14. It can be observed that the IAT of the energy-aware LPN is better than the unaware LPN. The DL data latency for the unaware LPN is better on the west side but experiences around 30 % of packet loss. The packets that waited longer in the queue are lost, and so the latency drops. However, when the discard percentage for both the LPNs are nearly equal (East side), we can observe that the energy-aware LPN performs better in terms of DL latency that is 34% low. The energy-aware LPN experiences two restarts that occur at 07:34 and 19:40 when the light illumination is low. We also tested the same setup with a 0.47 mF capacitor, and the results were similar but showing more restarts for the energy-unaware LPN, up to 115 on the east side. Being a sunny day, the capacitor voltage is maintained in the range between V_{max} and 4.45 V for almost the entire day, except during the sunrise and sunset. We present the variation in the capacitor voltage over the entire day of 10th July 2021, which was mostly cloudy and rainy. The sun rose and set at 05:39 AM and 09:56 PM [31]. The change in voltage for the energy-aware LPN's capacitor of 1 mF placed on both sides is measured for the whole day as shown in Figure 15. It can be observed that the east-side

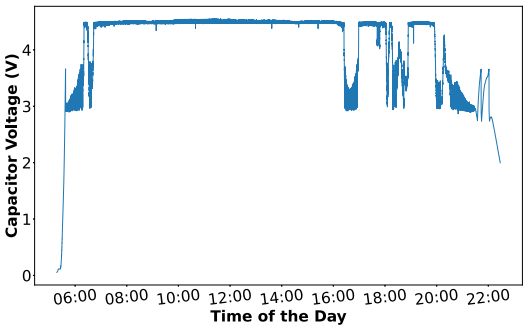

(a) East-Side LPN

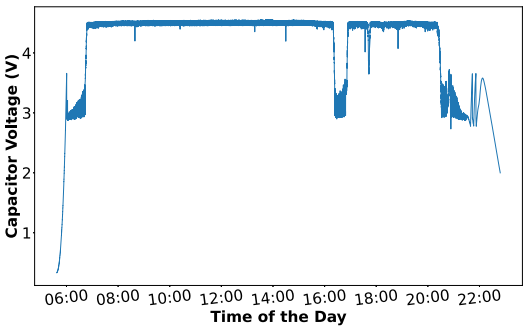

(b) West-Side LPN

Fig. 15. Variation in energy-aware LPN capacitor (1 mF) voltage over time with solar panel at the east and west side windows.

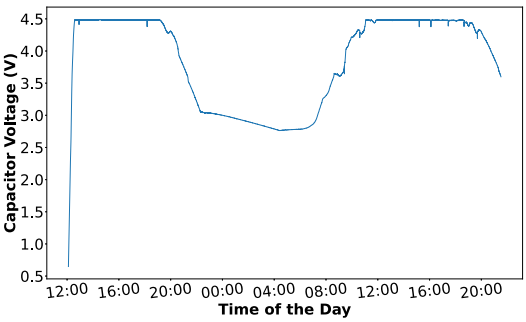

Fig. 16. Variation in energy-aware LPN capacitor (220 mF) voltage over two days with solar panel at the east side window.

LPN starts communication 22 min earlier than the west side (06:00) because it receives more light beforehand. Whereas during the sunset, the east side LPN turns off at 22:08, which is 21 minutes earlier than the west side, which was getting more light during the sunset. This also provides the west-side LPN a bit of power to reboot 3 times before turning off. Moreover, a sharp voltage down is observed after 16:20, which is due to heavy rainfall [32]. Apart from that, the capacitors maintain the V_{max} for almost the entire day.

However, when increasing the capacitor size to 220 mF in the east side LPN, it can be observed from Figure 16 that the capacitor voltage never drops below $V_{turnoff}$. It means the energy stored in a 220 mF capacitor during the daytime is sufficient to keep the communication active during the nighttime after a sunny day, maintaining DL latency of 1.47 s.

V. Conclusion

In this paper, we presented a working prototype of the batteryless BLE LPN, which operates by harvesting power from indoor light and is sufficient to support many IoT use-cases. The energy-unaware and aware LPN are compared for different capacitor sizes and harvesting powers. It can be concluded that the aware LPN performs better when configured by optimally choosing the energy check interval (ECI) values. This is because the ECI defines the time gap for the energy-aware LPN to recheck the available voltage if its capacitor voltage exceeds the required threshold value to execute a task successfully. The energy-aware LPN provides good performance with different friend queue sizes and different harvesting powers, communicating uni-or bi-directional data. At the harvesting power 140 μW and the friend queue size of 2, the energy-aware LPN avoids packet loss, which was around 47% for the energy-unaware LPN. The energy-aware LPN also shows improvement in DL data latency by 63% when receiving uni-directional DL data, and this improvement is increased to 74% when it performs bi-directional communication. With bi-directional communication, both the LPNs consumes a bit more energy to send the UL data and therefore, the overall DL latency for the corresponding harvesting power increases. The aware LPN also shows better performance results when it harvests from indoor artificial or sunlight (in all weathers).

References

[1] D. Filippini, *Autonomous Sensor Networks: Collective Sensing Strategies for Analytical* (Springer Series on Chemical Sensors and Biosensors). Berlin, Germany: Springer, 2013.

[2] H. Ibrahim, A. Ilinca, and J. Perron, "Energy storage systems—Characteristics and comparisons," *Renew. Sustain. Energy Rev.*, vol. 12, no. 5, pp. 1221–1250, 2008.

[3] M. K. Mishu *et al.*, "Prospective efficient ambient energy harvesting sources for IoT-equipped sensor applications," *Electronics*, vol. 9, no. 9, p. 1345, Aug. 2020.

[4] Q. Liu, W. I. Jntema, A. Drif, P. Pawelczak, M. Zuniga, and K. S. Yildirim, "Perpetual Bluetooth communications for the IoT," *IEEE Sensors J.*, vol. 21, no. 1, pp. 829–837, Jan. 2021.

[5] *Mesh Profile Bluetooth Specifications*. Accessed: Sep. 30, 2021. [Online]. Available: https://www.bluetooth.com/specifications/mesh-specifications/

[6] A. K. Sultania, C. Delgado, and J. Famaey, "Enabling low-latency Bluetooth low energy on energy harvesting batteryless devices using wake-up radios," *Sensors*, vol. 20, no. 18, p. 5196, Sep. 2020.

[7] N. Radhika, P. Tandon, T. V. Prabhakar, and K. J. Vinoy, "RF energy harvesting for self powered sensor platform," in *Proc. 16th IEEE Int. New Circuits Syst. Conf. (NEWCAS)*, Montreal, QC, Canada, Jun. 2018, pp. 24–27.

[8] T. Sanislav, S. Zeadally, G. D. Mois, and S. C. Folea, "Wireless energy harvesting: Empirical results and practical considerations for Internet of Things," *J. Netw. Comput. Appl.*, vol. 121, pp. 149–158, Nov. 2018.

[9] F. Fraternali, B. Balaji, Y. Agarwal, L. Benini, and R. Gupta, "Pible: Battery-free mote for perpetual indoor BLE applications," in *Proc. 5th Conf. Syst. Built Environ.*, Shenzen, China, Nov. 2018, pp. 168–171.

[10] M. Meli and M. Würth, "Advertising position with battery-less Bluetooth low energy," in *Proc. Embedded World Conf.*, Nuremberg, Germany, Mar. 2012, pp. 1–13.

[11] M. Meli and M. Würth, "Indoor battery-less temperature and humidity sensor for Bluetooth low energy," in *Proc. Wireless Congr.*, Munich, Germany, Nov. 2011, pp. 1–9.

[12] T. Wu, J.-M. Redoute, and M. R. Yuce, "Subcutaneous solar energy harvesting for self-powered wireless implantable sensor systems," in *Proc. 40th Annu. Int. Conf. IEEE Eng. Med. Biol. Soc. (EMBC)*, Honolulu, HI, USA, Jul. 2018.

[13] K. E. Jeon, J. She, J. Xue, S. Kim, and S. Park, "luXbeacon—A batteryless beacon for green IoT: Design, modeling, and field tests," *IEEE Internet Things J.*, vol. 63, no. 3, pp. 5001–5012, Jun. 2019.

[14] H.-D. Jang, "Study on design method of energy harvesting system for BLE beacon," *J. Korean Inst. Commun. Inf. Sci.*, vol. 42, no. 1, pp. 149–152, Jan. 2017.

[15] H. D. Jang, "Study on the design method of the energy harvesting smart sensor for implementing IoT service," *J. Korea Inst. Inf., Electron., Commun. Technol.*, vol. 11, no. 1, pp. 89–94, 2018.
[16] Y. Zhong *et al.*, "Development of an implantable wireless and batteryless bladder pressure monitor system for lower urinary tract dysfunction," *IEEE J. Transl. Eng. Health Med.*, vol. 8, pp. 1–7, 2020.
[17] O. Witham, L. N. Johnston, M. Xiao, J. Feng, N. Zhou, and G. Shaker, "Batteryless wireless water leak detection system," in *Proc. Int. Conf. Smart Appl., Commun. Netw. (SmartNets)*, Sharm El Sheik, Egypt, Dec. 2019, pp. 1–4.
[18] T. Ruan, Z. J. Chew, and M. Zhu, "Energy-aware approaches for energy harvesting powered wireless sensor nodes," *IEEE Sensors J.*, vol. 17, no. 7, pp. 2165–2173, Apr. 2017.
[19] *AEM10941 Solar Energy Harvesting*. Accessed: Sep. 30, 2021. [Online]. Available: https://e-peas.com/product/aem10941/
[20] R. Yan, H. Sun, and Y. Qian, "Energy-aware sensor node design with its application in wireless sensor networks," *IEEE Trans. Instrum. Meas.*, vol. 62, no. 5, pp. 1183–1191, May 2013.
[21] B. Srbinovski, M. Magno, B. O'Flynn, V. Pakrashi, and E. Popovici, "Energy aware adaptive sampling algorithm for energy harvesting wireless sensor networks," in *Proc. IEEE Sensors Appl. Symp. (SAS)*, Apr. 2015, pp. 1–6.
[22] *Power Profiler Kit II*. Accessed: Sep. 30, 2021. [Online]. Available: https://www.nordicsemi.com/Products/Development-hardware/Power-Profiler-Kit-2
[23] S. Bunjongjit, A. Ngaopitakkul, and M. Leelajindakrairerk, "Analysis of harmonics in indoor lighting system with LED and fluorescent luminaire," in *Proc. IEEE 3rd Int. Future Energy Electron. Conf. ECCE Asia (IFEEC-ECCE Asia)*, Kaohsiung, Taiwan, Jun. 2017, pp. 3–7.
[24] J. Bernegger and M. Meli, "Comparing the energy requirements of current Bluetooth smart solutions," in *Proc. Embedded World Conf.*, Nuremberg, Germany, Feb. 2014, pp. 25–27.
[25] *nRF52840 DK*. Accessed: Sep. 30, 2021. [Online]. Available: https://www.nordicsemi.com/Products/Development-hardware/nrf52840-dk
[26] *Low Power Node Example*. Accessed: Sep. 30, 2021. [Online]. Available: https://infocenter.nordicsemi.com/topic/com.nordic.infocenter.meshsdk.v4.2.0/md_examples_lpn_README.html
[27] *Light Switch Example*. Accessed: Sep. 30, 2021. [Online]. Available: https://infocenter.nordicsemi.com/topic/com.nordic.infocenter.meshsdk.v4.2.0/md_examples_light_switch_README.html
[28] *Voltage Divider Calculator*. Accessed: Sep. 30, 2021. [Online]. Available: https://www.allaboutcircuits.com/tools/voltage-divider-calculator/
[29] A. Sabovic, C. Delgado, D. Subotic, B. Jooris, E. De Poorter, and J. Famaey, "Energy-aware sensing on battery-less LoRaWAN devices with energy harvesting," *Electronics*, vol. 9, no. 6, p. 904, May 2020.
[30] T. Olofsson, "Energy harvesting with solar cells for wireless alarm nodes," Fac. Eng., Lund Univ., Lund, Sweden, Tech. Rep. 8959130, 2018.
[31] *Antwerp Historical Weather, BE*. Accessed: Sep. 30, 2021. [Online]. Available: https://www.worldweatheronline.com/antwerp-weather-history/be.aspx
[32] *Past Weather in Antwerp, Belgium*. Accessed: Sep. 30, 2021. [Online]. Available: https://www.timeanddate.com/weather/belgium/antwerp/historic/

Ashish Kumar Sultania received the B.E. degree in information technology from the University of Delhi, India, in 2011, and the M.Sc. degrees in computer science from the University of Tartu, Estonia, and the Norges Teknisk-Naturvitenskapelige Universitet, Norway, in 2017. He is currently a Ph.D. Researcher with the University of Antwerp—imec, Belgium. Prior to starting his master's, degree he worked as a Senior Software Engineer at NXP Semiconductor, India, from 2011 to 2015. His research focuses on optimizing the energy consumption of IoT devices and their networks.

Jeroen Famaey (Senior Member, IEEE) received the M.Sc. and Ph.D. degrees in computer science from Ghent University, Belgium, in 2007 and 2012, respectively. Since 2016, he has been a Research Professor associated with the University of Antwerp—imec, Belgium. He has coauthored over 130 articles published in international peer-reviewed journals and conference proceedings and ten patent applications (five of which have been granted). His research contributions have resulted in several awards, among which five best paper awards. He has participated in over 20 international and national research projects, both fundamental and industry-driven. His current research interests include network performance modeling and optimization, low-power wireless networks with energy harvesting, and mmWave- and THz-band networking.